Microfabricated vapor cell atomic clocks

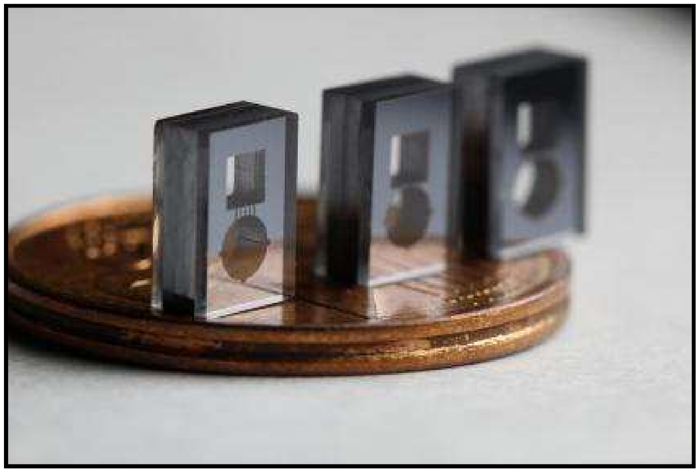

R. Boudot

FEMTO-ST, CNRS, Besançon, France

rodolphe.boudot@femto-st.fr
http://teams.femto-st.fr/equipe-ohms/
http://teams.femto-st.fr/MOSAIC/en

Funded by the European Union

Atomic clocks

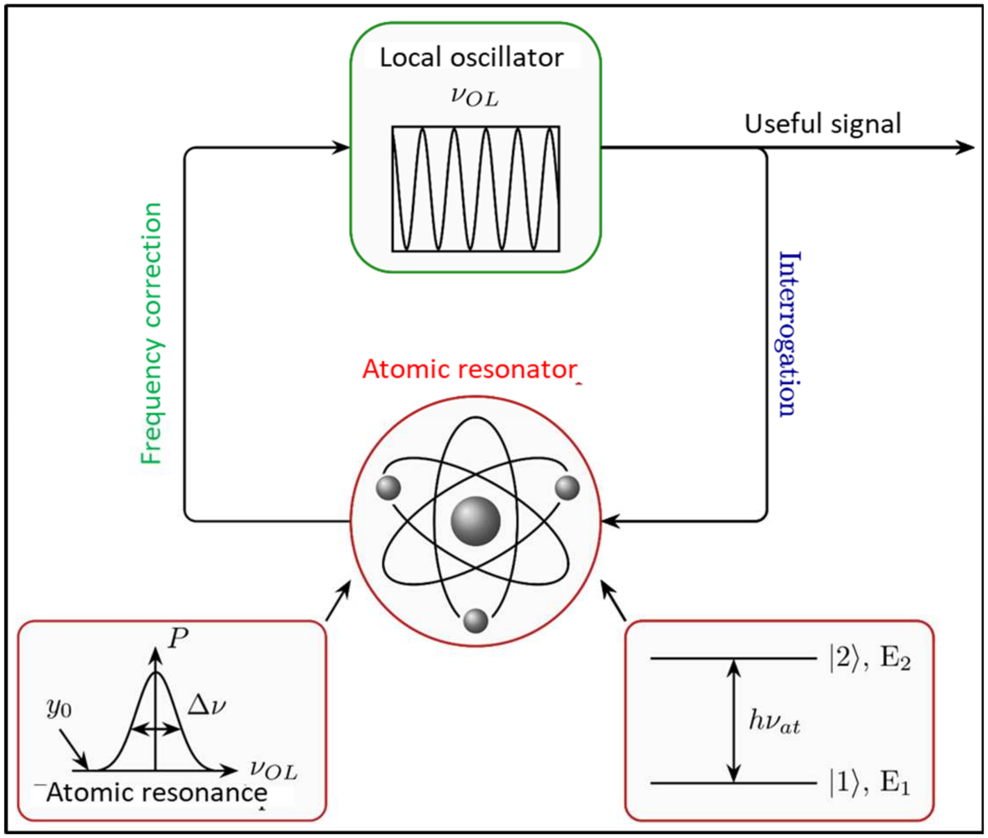

The local oscillator (LO) frequency
is stabilized onto the atomic transition

Short-term stability

$$\sigma_y(\tau) = \frac{\Delta\nu}{\nu_0}\frac{1}{S/N}\tau^{-1/2}$$

Δν: linewidth
ν_0: transition frequency
S/N: signal-to-noise ratio (1Hz BW)
τ: integration time

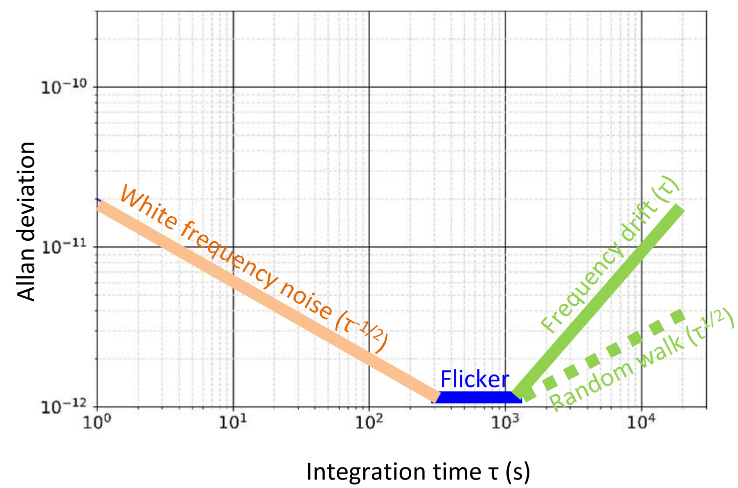

Long-term stability
Sensitivity of the clock frequency
to experimental parameters
(temperature, B-field, laser power,..)

Motivation: high-stability miniaturized atomic clocks

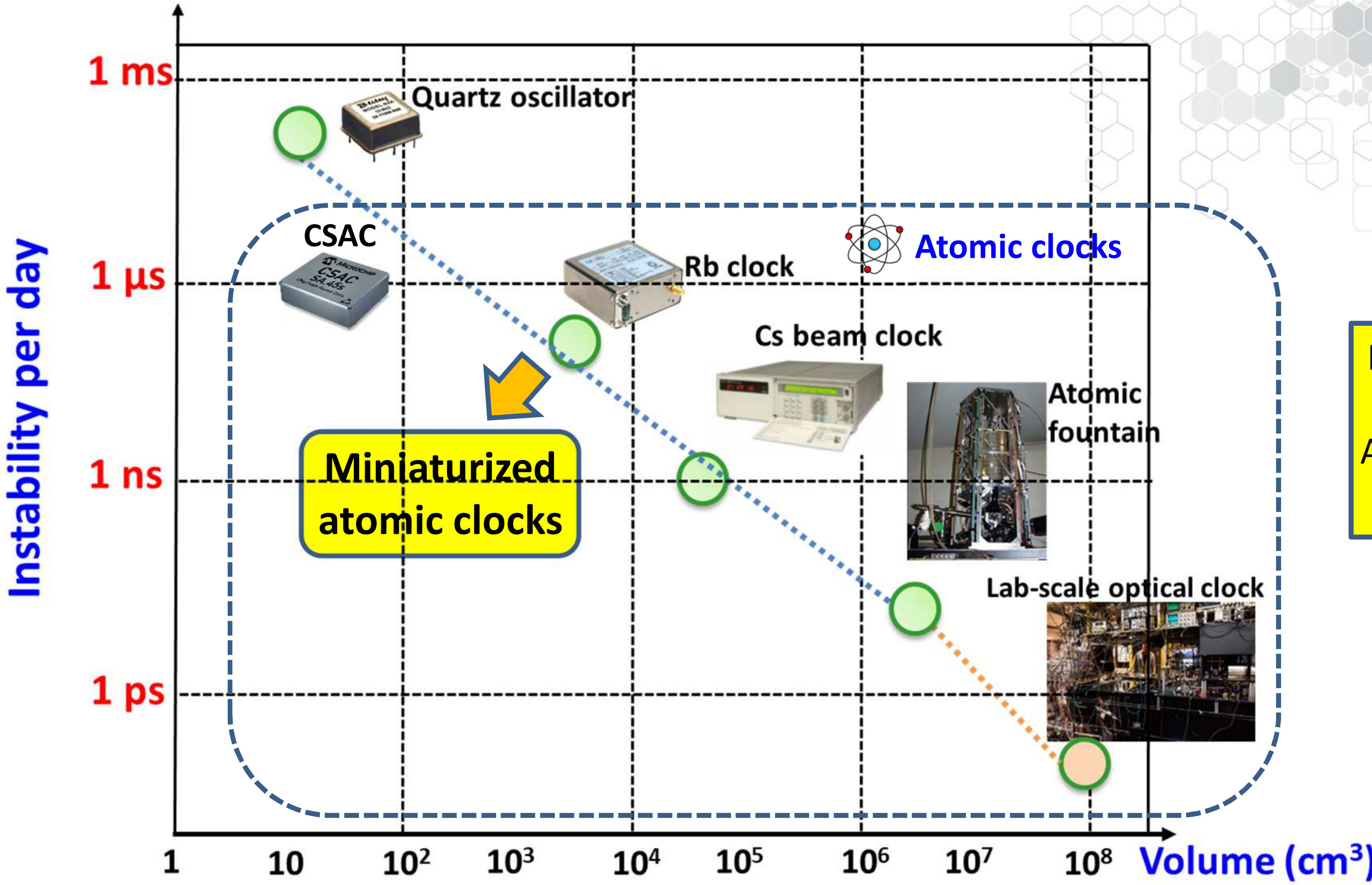

MEMS technologies
Photonics
Atomic spectroscopy
Metrology

Applications

20th birthday of the first chip-scale atomic clock (CSAC)

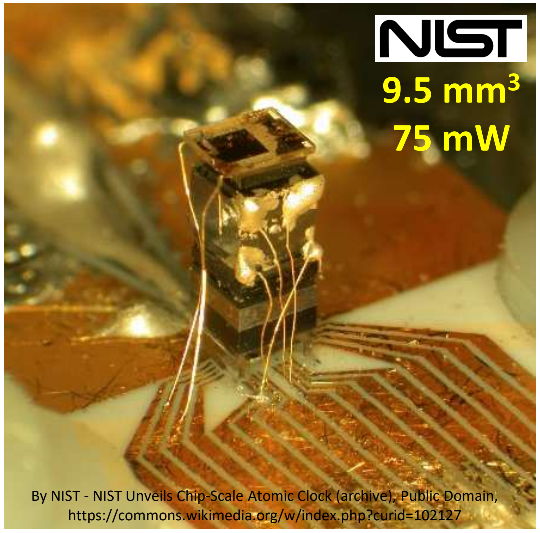

S. Knappe et al., Appl. Phys. Lett. 85, 9 (2004)

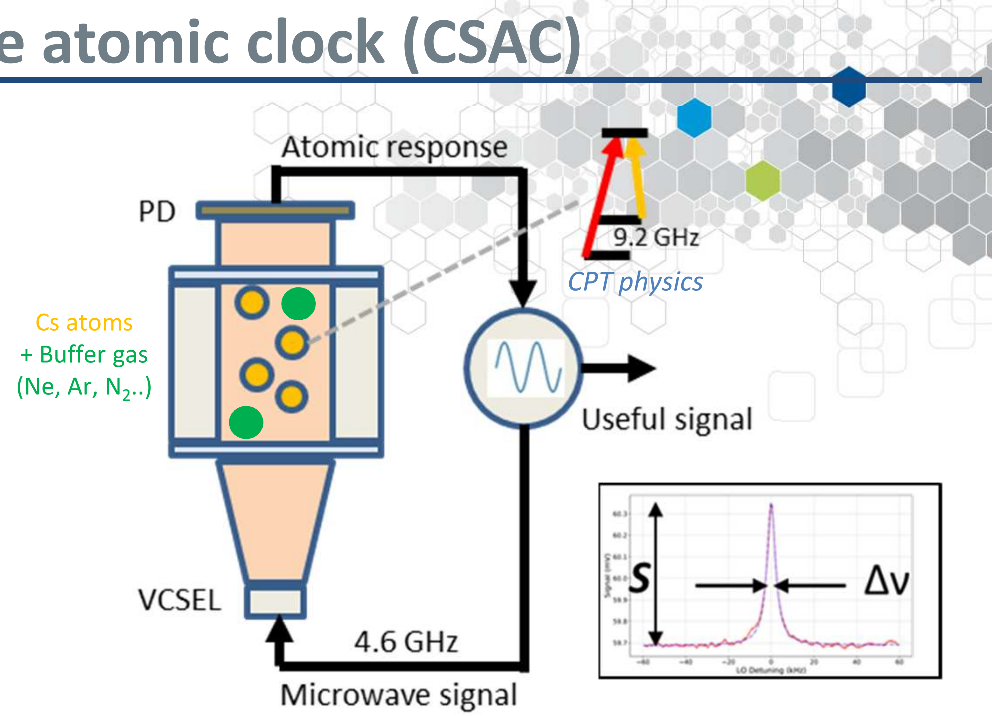

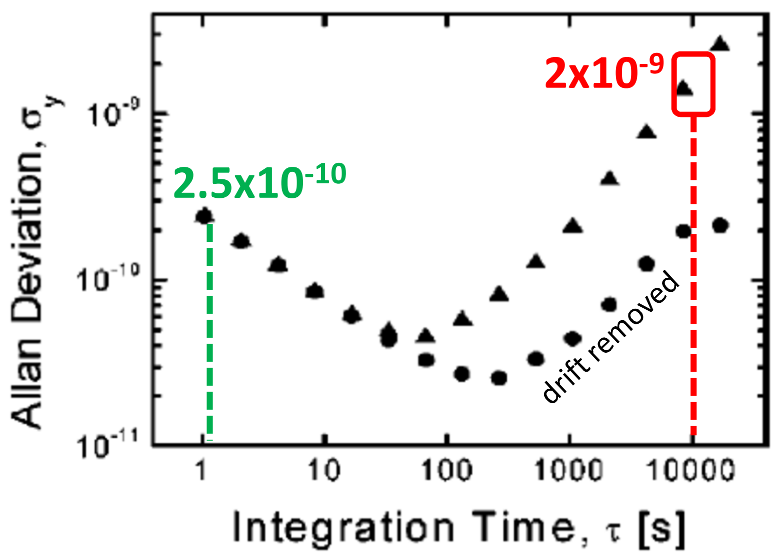

CPT-based microcell clocks worldwide

Low power miniaturized clocks

Volume < 20 cm^3
Embedded devices

Consumption < 150 mW
Longer battery-powered missions

Operating temperature - 40 à 85°C
Compliant with industrial standards

Frequency stability 10^{-11} at 1 h and 1 day
Timing error < 1 µs/day

J. Kitching et al., Appl. Phys. Rev. 5, 031202 (2018)

100 times more stable than OCXOs in a comparable size-power budget

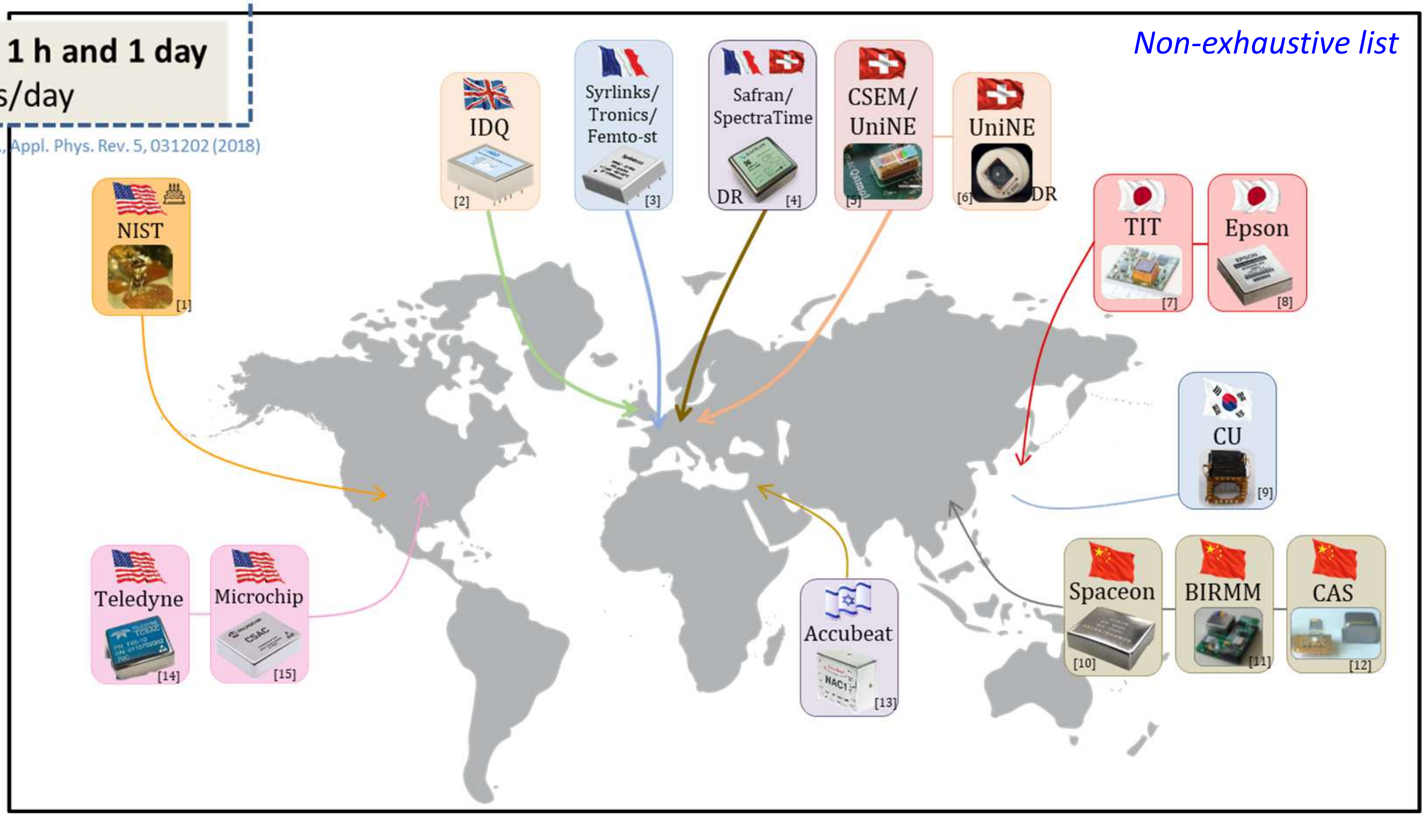

Cell technology and physics packages

Cs MEMS cell technology

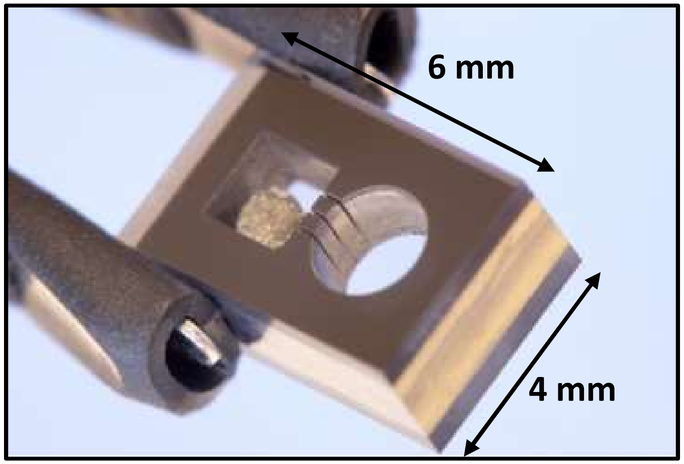

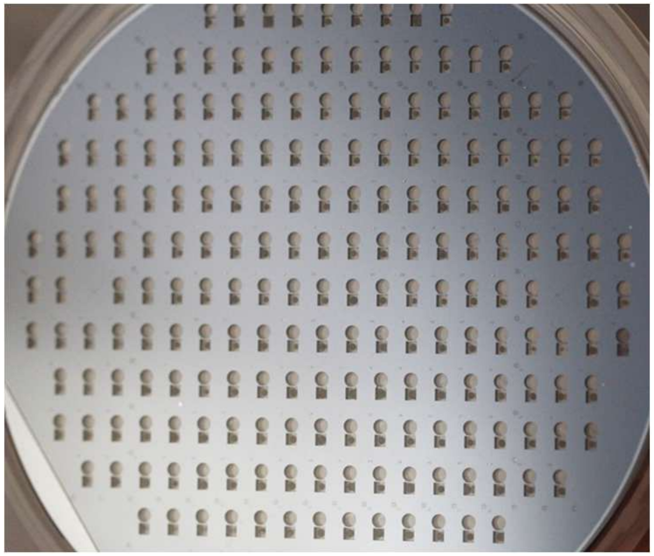

A. Douahi et al., Elec. Lett. 43, 5, 279 (2007)
M. Hasegawa et al., Sens. Act. 167, 594 (2011)
V. Maurice et al., Appl. Phys. Lett. 110, 164103 (2017)

Integrated physics packages

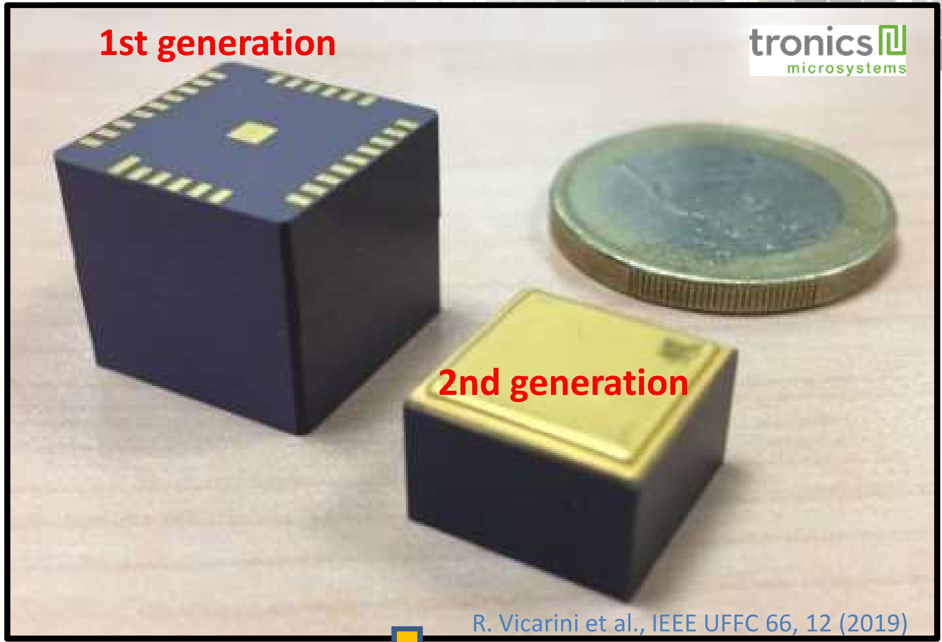

First prototype Industrial french CSAC (2018)

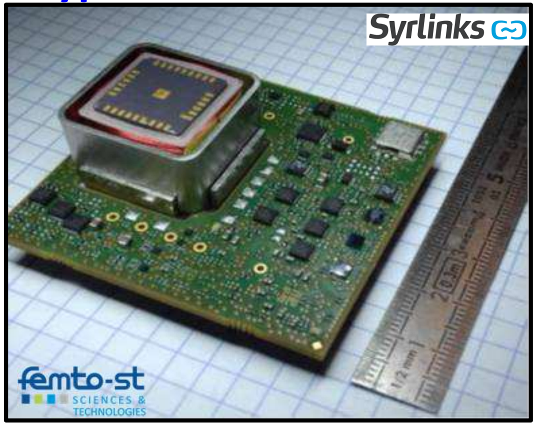

https://www.syrlinks.com/en/time-frequency/mems-micro-atomic-clock-mmac/mems-micro-atomic-clock-mmac

Limitations of a CPT-based microcell clock

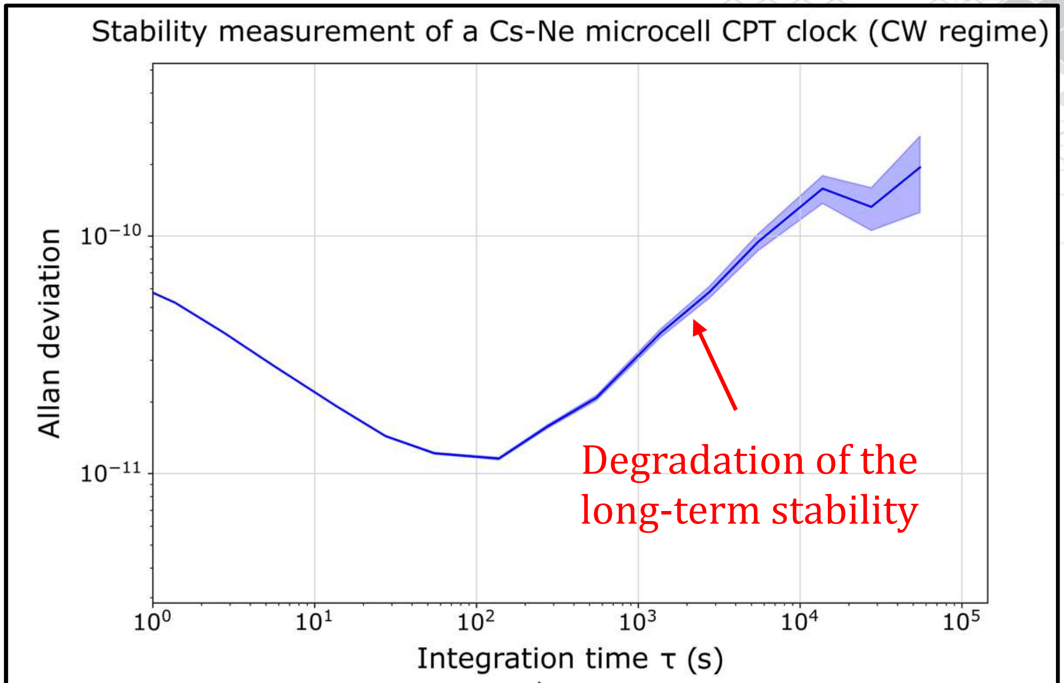

Long-term stability limited by 2 main contributions

Light-shift effects
(laser power, microwave power variations, etc.)

Ramsey-based interrogation protocols
(Reduction of light-shifts)

Buffer gas pressure shift
(cell atmosphere evolution)

Advanced MEMS cell technology
(Improved purity and stability)

Ramsey-CPT spectroscopy for light-shift mitigation

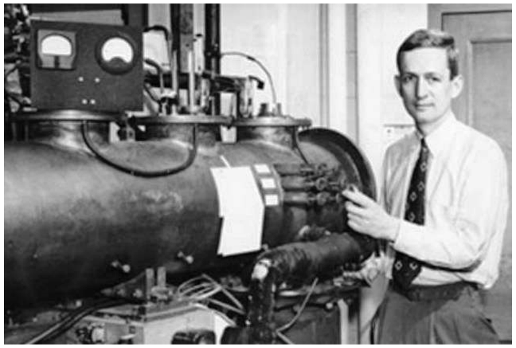

N. F. Ramsey, Phys. Rev. **78**, 695 (1950)

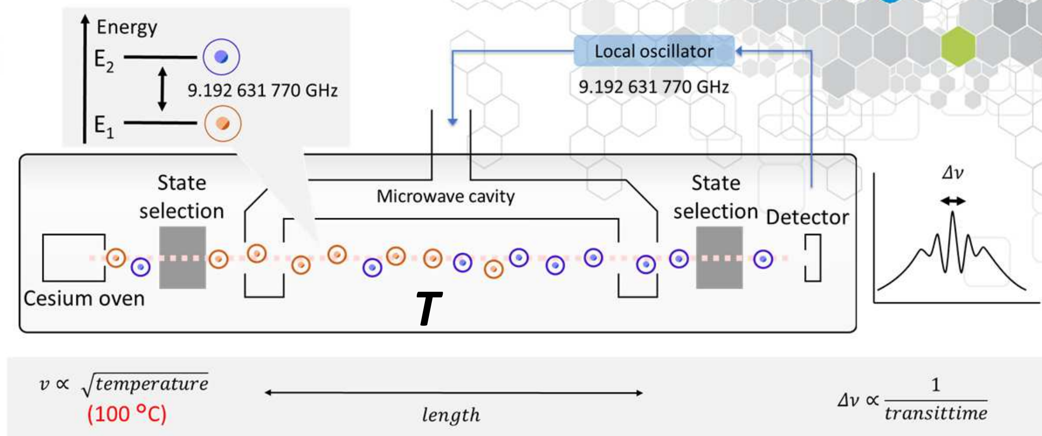

Two atom-field interactions separated by a free-evolution time *T* ➡ *Ramsey fringes*

Ramsey-CPT spectroscopy in a MEMS cells

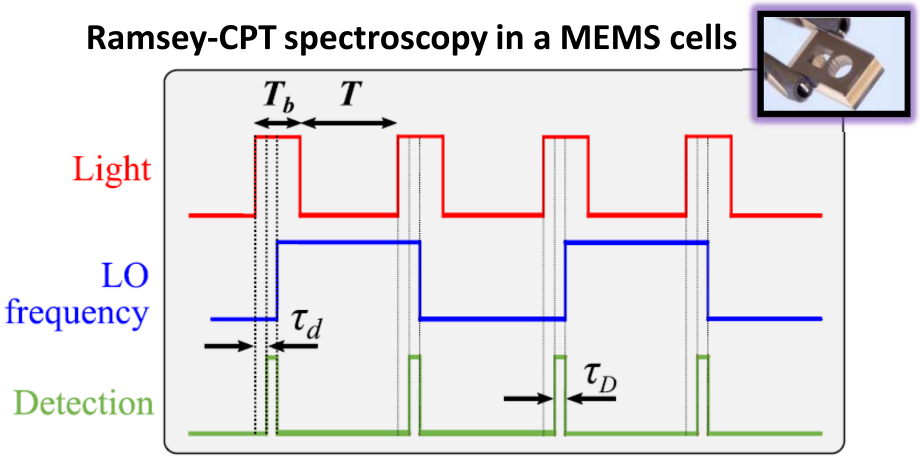

Typical sequence : T_b = 150 µs, T = 150 µs, τ_d = 10 µs, τ_D = 10 µs

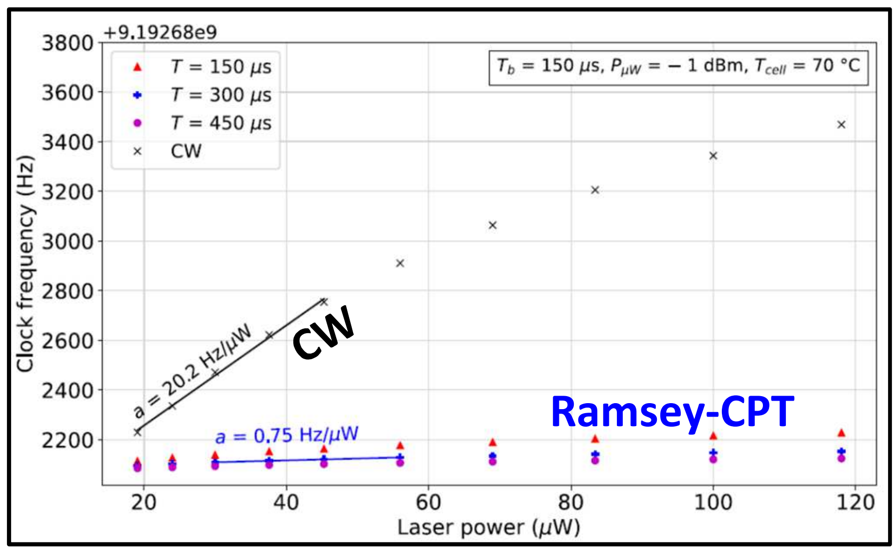

C. Carlé *et al.*, IEEE UFFC **68**, 10 (2021)

Symmetric Auto-Balanced Ramsey (SABR) interrogation

Residual sensitivity to light shifts produced during the pulses

⇩

Auto-Balanced Ramsey spectroscopy

C. Sanner et al., Phys. Rev. Lett. 120, 053602 (2018)

Compensate the phase shift experienced by the atoms during the pulses by applying a phase correction to the LO during the dark time T

⇩

Apply two consecutive Ramsey cycles with different dark times (short T_s and long T_L)

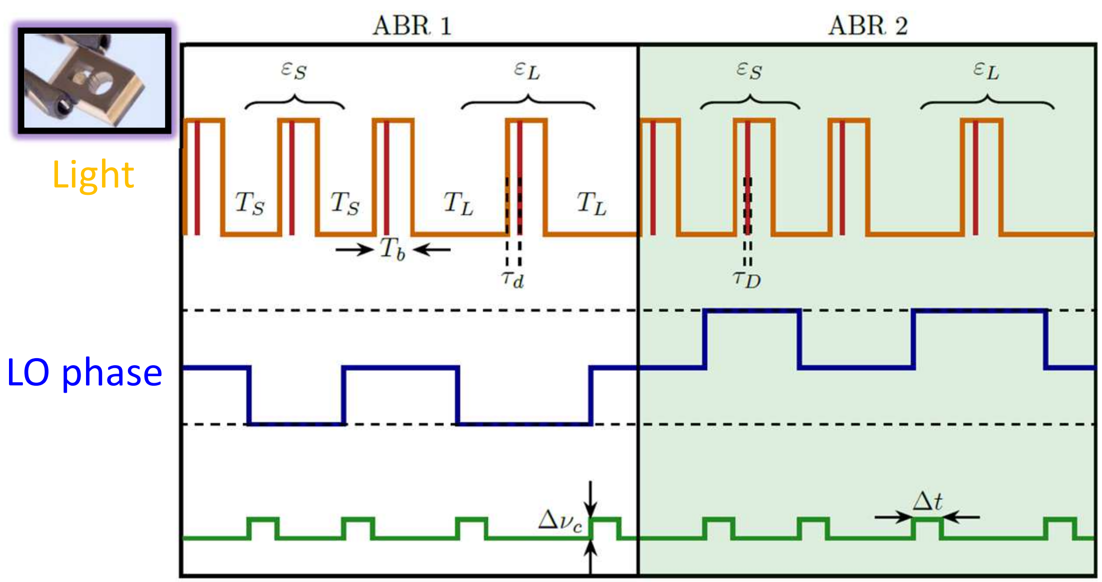

Symmetric Auto-Balanced Ramsey interrogation in MEMS vapor cells

Symmetric ABR in MEMS cells

T_b = 150 µs, T_S = 100 µs, T_L = 250 µs τ_d = 10 µs, τ_D = 10 µs

⇩

Error signals

$$\begin{cases} \varepsilon_+ = \varepsilon_S + \varepsilon_L \\ \varepsilon_- = \varepsilon_S - \varepsilon_L \end{cases}$$

- ε_+ ⇨ **LO frequency**
- ε_- ⇨ **Light-shift mitigation**

M. Abdel Hafiz et al., Appl. Phys. Lett. 120, 064101 (2022)

Light-shift mitigation with SABR-CPT in MEMS cells

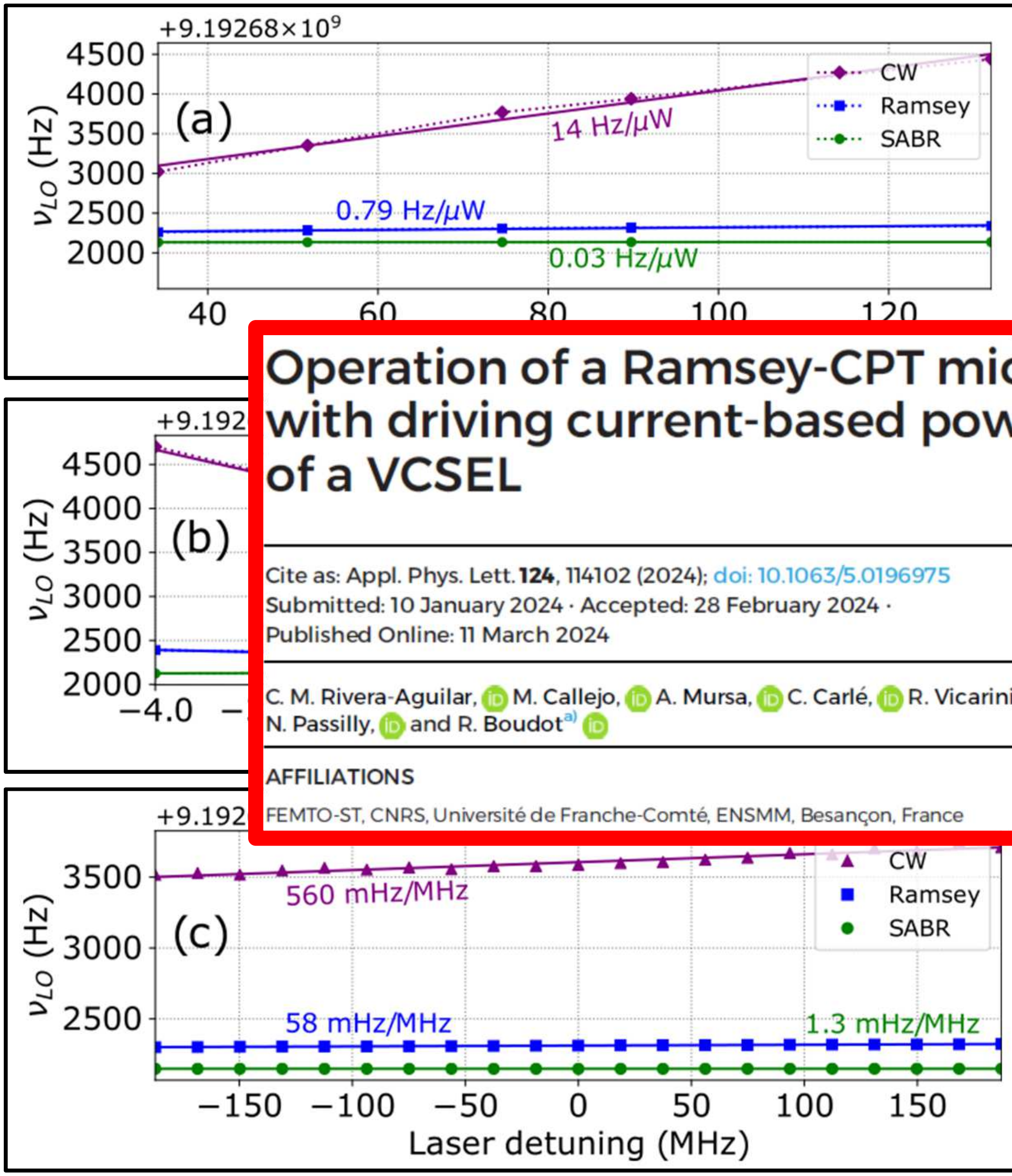

Operation of a Ramsey-CPT microcell atomic clock with driving current-based power modulation of a VCSEL

Cite as: Appl. Phys. Lett. **124**, 114102 (2024); doi: 10.1063/5.0196975
Submitted: 10 January 2024 · Accepted: 28 February 2024 ·
Published Online: 11 March 2024

View Online Export Citation CrossMark

C. M. Rivera-Aguilar, M. Callejo, A. Mursa, C. Carlé, R. Vicarini, M. Abdel Hafiz, J.-M. Friedt, N. Passilly, and R. Boudot[a)]

AFFILIATIONS
FEMTO-ST, CNRS, Université de Franche-Comté, ENSMM, Besançon, France

Laser power
Sensitivity reduced by:
466 (Vs CW)
17 (Vs Ramsey)

Sensitivity reduced by:
430 (Vs CW)
10 (Vs Ramsey)

M. Abdel Hafiz *et al*, App. Phys. Lett., 120, 064101 (2022)

First clock stability tests with SABR

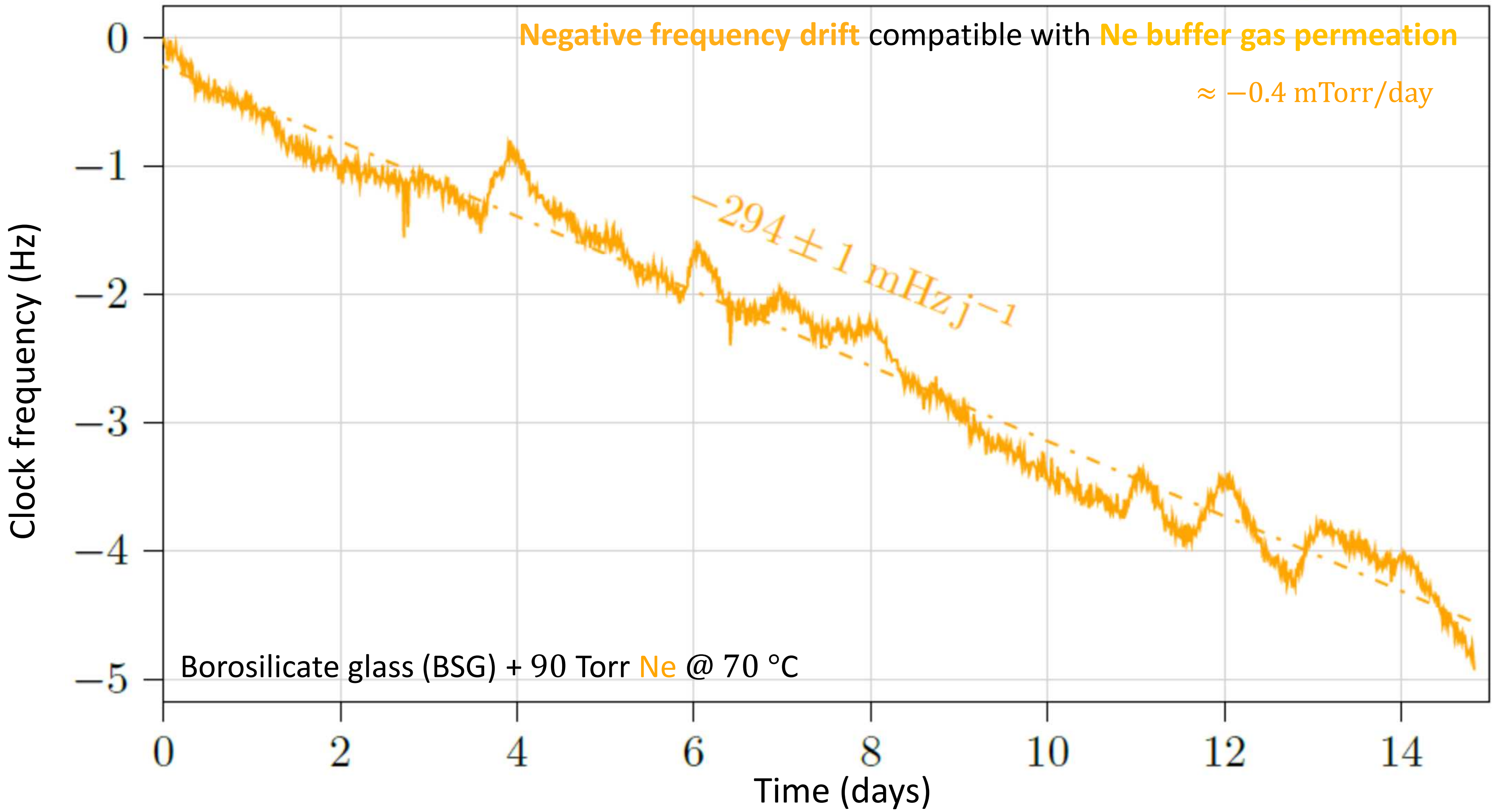

Dedicated studies on gas permeation

S. Abdullah et al. Appl. Phys. Lett. **106**, 101063 (2015)

Gas permeation through the cell walls

Buffer gas induces a shift $\Delta\nu_{bg}$ of the clock transition frequency :

$$\Delta\nu_{bg} = P[\beta + \delta(T - T_0) + \gamma(T - T_0)^2]$$

Buffer gas can enter into or leave the cell

($\beta_{Ne} = 686$ Hz/Torr , $\Delta P/P \approx 10^{-7}$ to reach a stability of 10^{-12})

β, δ, γ: gas coefficients
T: cell temperature
T_0: ref. temperature (273.16K)
P: total pressure (at 0°C)

Evolution of the buffer gas pressure

$$P(t) = P_{ext} - (P_{ext} - P_{in}) \times e^{-\frac{t}{\tau}}$$

$$\tau = \frac{V \times d}{K \times A \times P_{ref}}$$

K: **permeation rate**

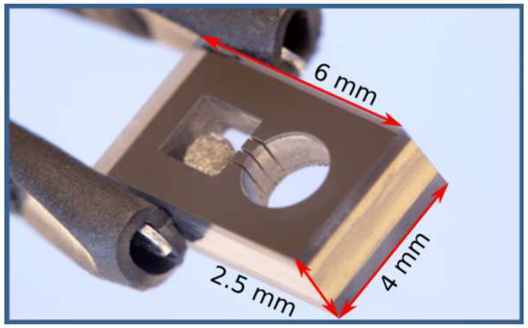

Clock frequency evolution ⇨ Buffer gas pressure evolution ⇨ K

V = volume, d = thickness, A = surface, P_{ref} = Atm. Pres. et P_{in}, P_{ext} = Press. in and out of the membrane

Gas permeation: BSG Vs ASG (tests with He buffer gas)

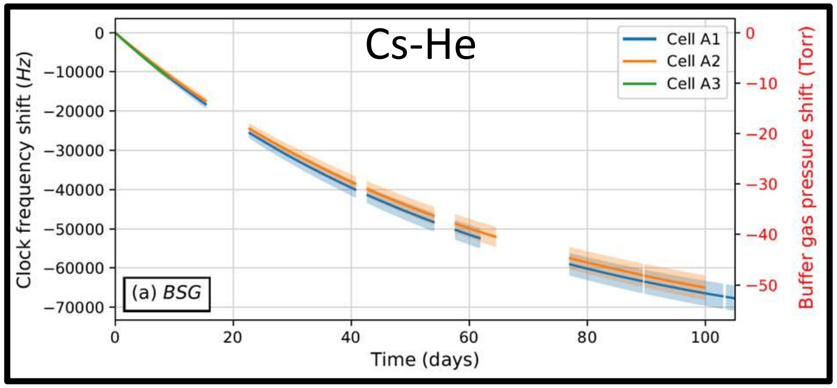

Loss of 50 torrs of He in 3 months

Exponential fit in agreement with permeation process

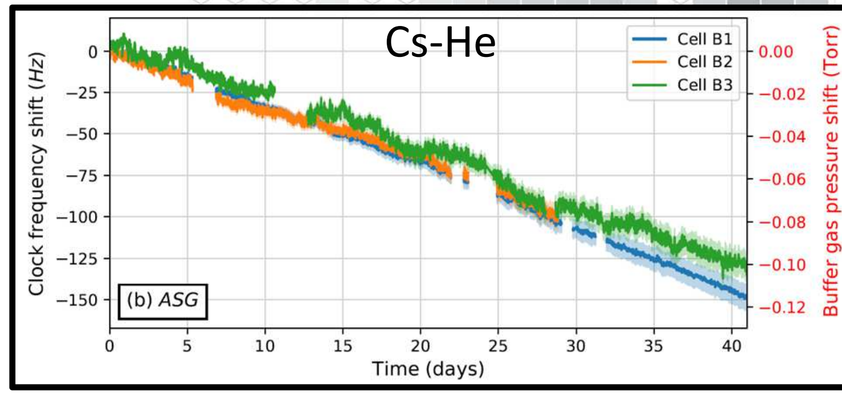

Permeation rate reduced by ~ 450

In agreement with [2]

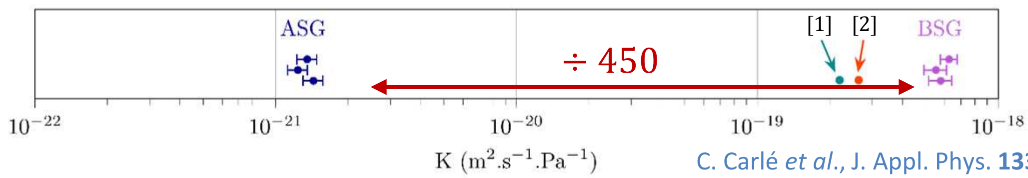

C. Carlé *et al.*, J. Appl. Phys. **133**, 214501 (2023)

Providers of wafer-compatible ASG are rare

Composition	ASG (%)	BSG (%)
Al_2O_3	25	2
SiO_2	60	81
B_2O_3	2	13
NaO_2	10	4

[1] S. Abdullah et al., Appl. Phys. Lett. **106**, 101063 (2015)
[2] A. Dellis et al., Opt. Lett. **41**, 12 (2016)

Gas permeation: Al_2O_3 coatings (tests with He buffer gas)

Al_2O_3 coatings can be used to limit the alkali consumption by the glass

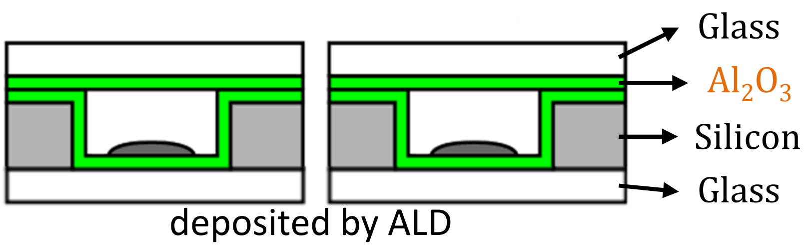

S. Woetzel et al., Surf. Coat. Tech. 221, 158 (2013)
S. Karlen et al., Opt. Exp. 25, 3, 2187 (2017)
G. Pate et al., Opt. Lett. 48, 2, 383 (2023)

Cs-He **BSG** + Al_2O_3 (20 nm)

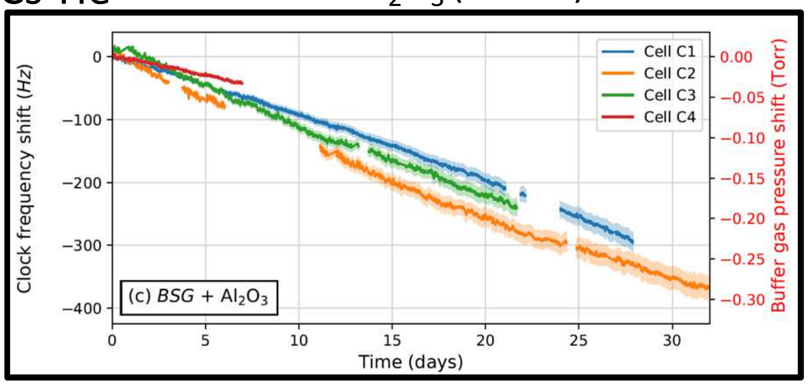

Cs-He **ASG** + Al_2O_3 (20 nm)

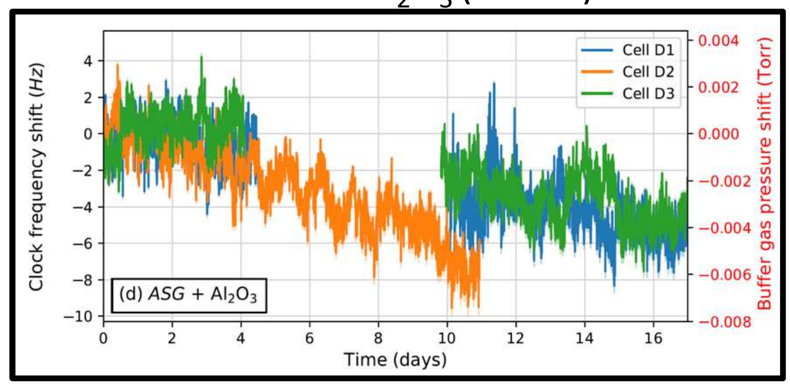

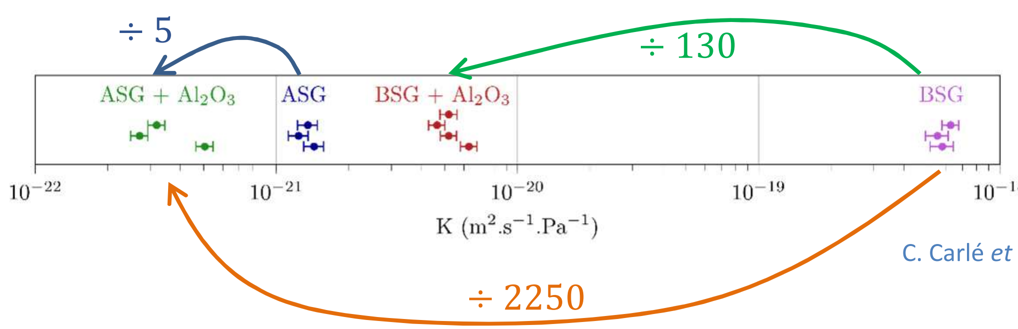

C. Carlé *et al.*, J. Appl. Phys. **133**, 214501 (2023)

Al_2O_3 reduces He permeation. Good alternative to ASG.

Impact of the Al_2O_3 coating thickness

10 cells BSG + Helium

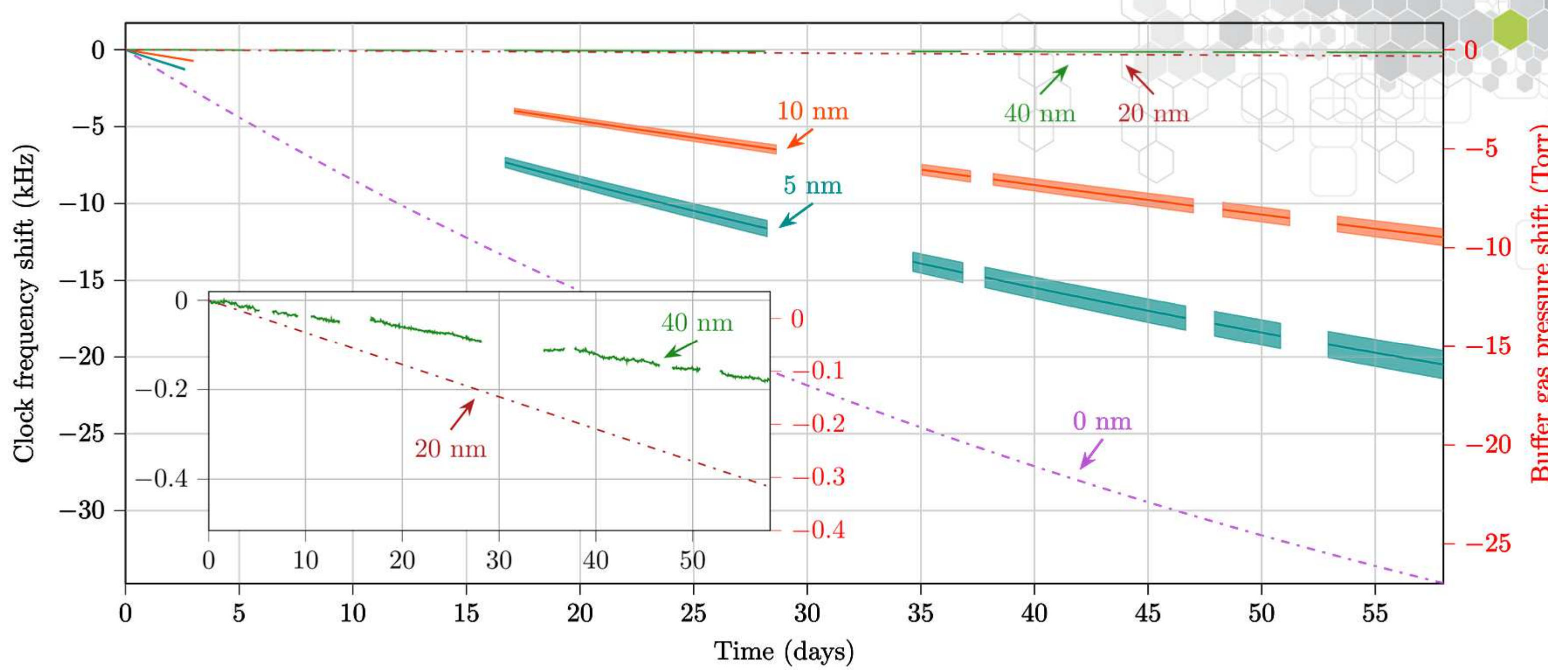

Permeation rate versus Al_2O_3 thickness

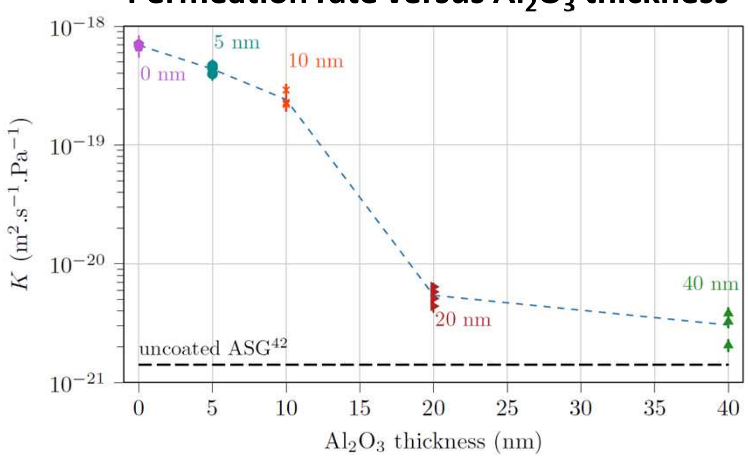

Reduction of He permeation until 20 nm

Not a significant improvement
between 20 and 40 nm

C. Carlé et al., ArXiv 2404.07144 (2024)
Accepted in J. Appl. Phys. (2024)

What about Ne permeation ?

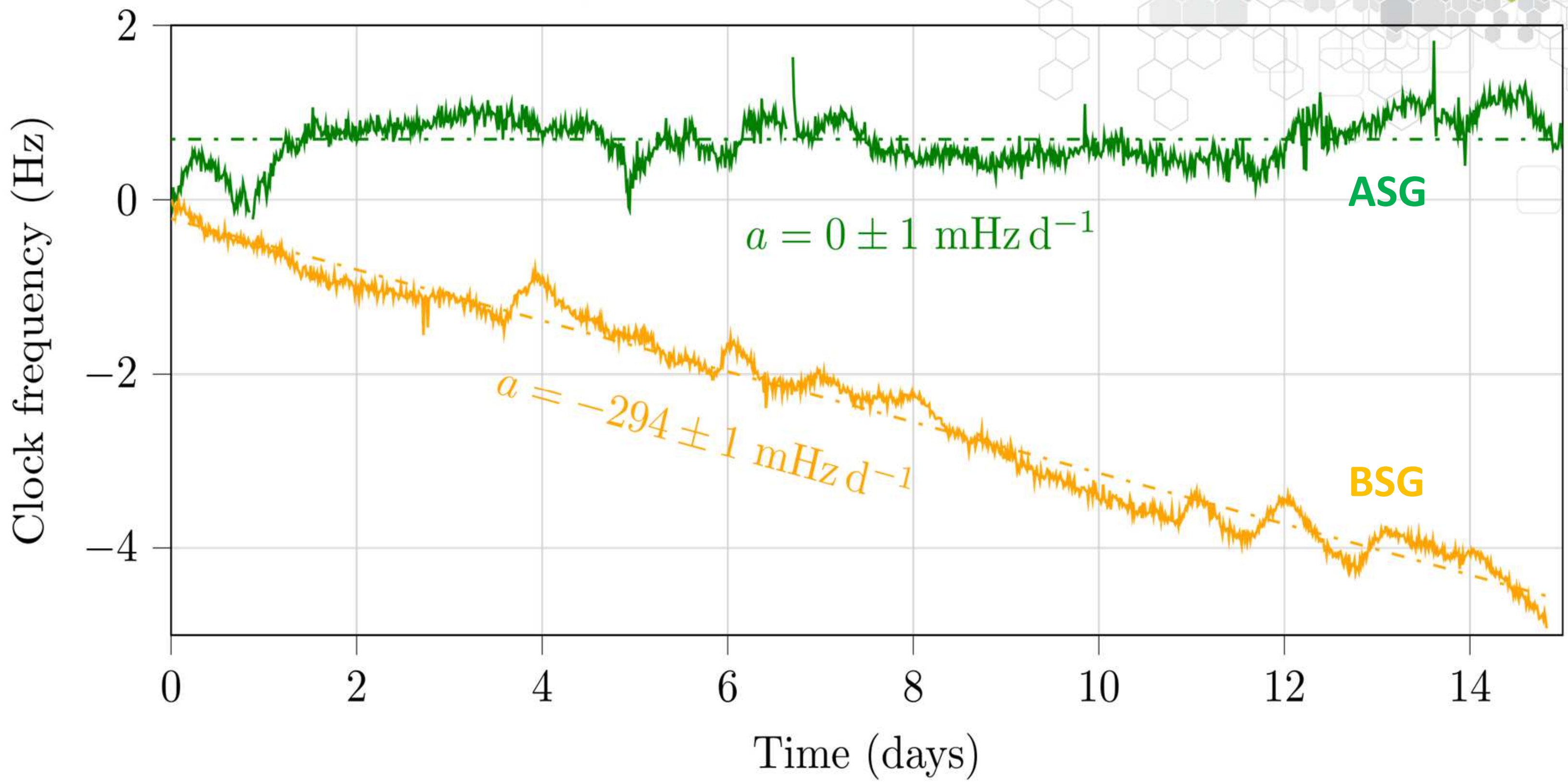

Strong reduction of Ne permeation with ASG

C. Carlé *et al.*, Opt. Exp. 31, 5, 8160 (2023)

Also observed with Al_2O_3 coatings

C. Carlé et al., ArXiv 2404.07144 (2024)

Accepted in J. Appl. Phys. (2024)

Stability results with a microcell Cs-Ne CPT clock (SABR + ASG)

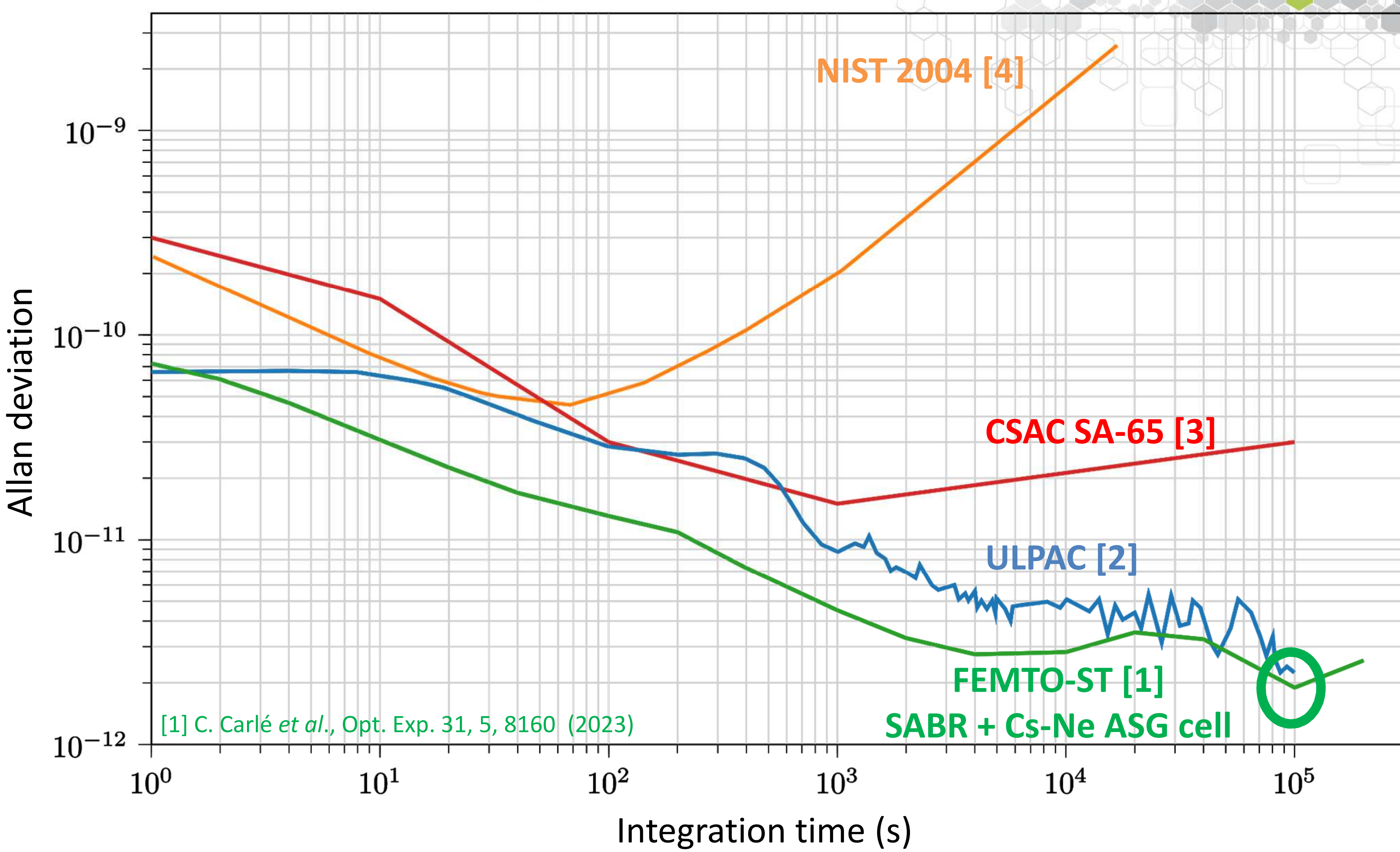

[2] H. Zhang *et al.*, IEEE J. Solid state (2019)
[3] Microchip CSAC SA65 datasheet
[4] S. Knappe *et al.*, Appl. Phys. Lett. **85**, 9 (2004).

Increased operation temperature with buffer gas mixtures

Neon: inversion temperature around **79°C** [1]

O. Kozlova et al. Phys. Rev. A **83**, 062714 (2011)

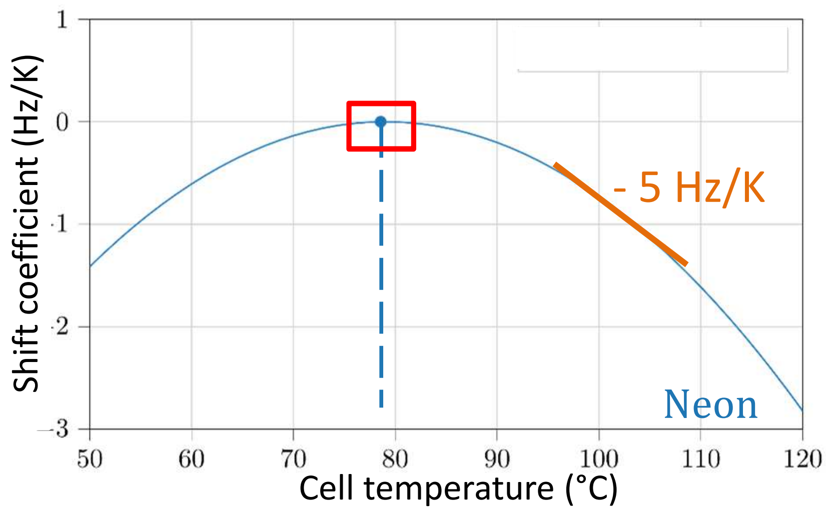

Cs cell with Ne-He mixture

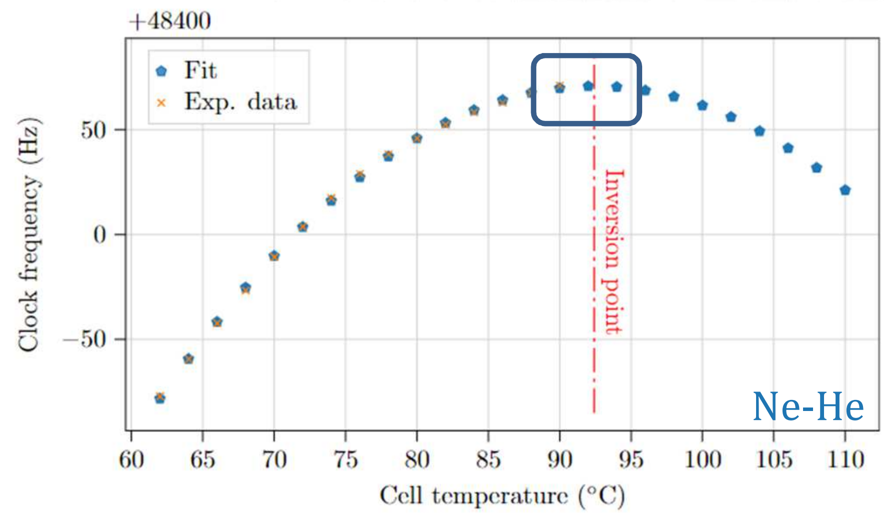

Some applications require the clock to operate at higher temperatures.

Reduction of He permeation with ASG

Cells with Ne-He mixture

Increase T_{inv}, fixed by the bg pressure ratio

Expected 4.7% He for T_{inv} = 100°C

$T_{inv} \approx 92.4$ °C

$\Downarrow$

$$\begin{cases} r_{He} = 3\ \% \\ r_{Ne} = 97\ \% \end{cases}$$

Lack of precision in the mixture ratio

Microcells with tunable He-Ne buffer gas mixtures

Use of break-seal gas reservoirs

Science cavity pre-filled with Ne
Non-through reservoirs pre-filled with He
He gas released through fs laser ablation of a wall membrane

V. Maurice et al., Nature Microsystems and Nanoengineering 8, 129 (2022)

N_2-based mixtures

Break-seals and make-seals

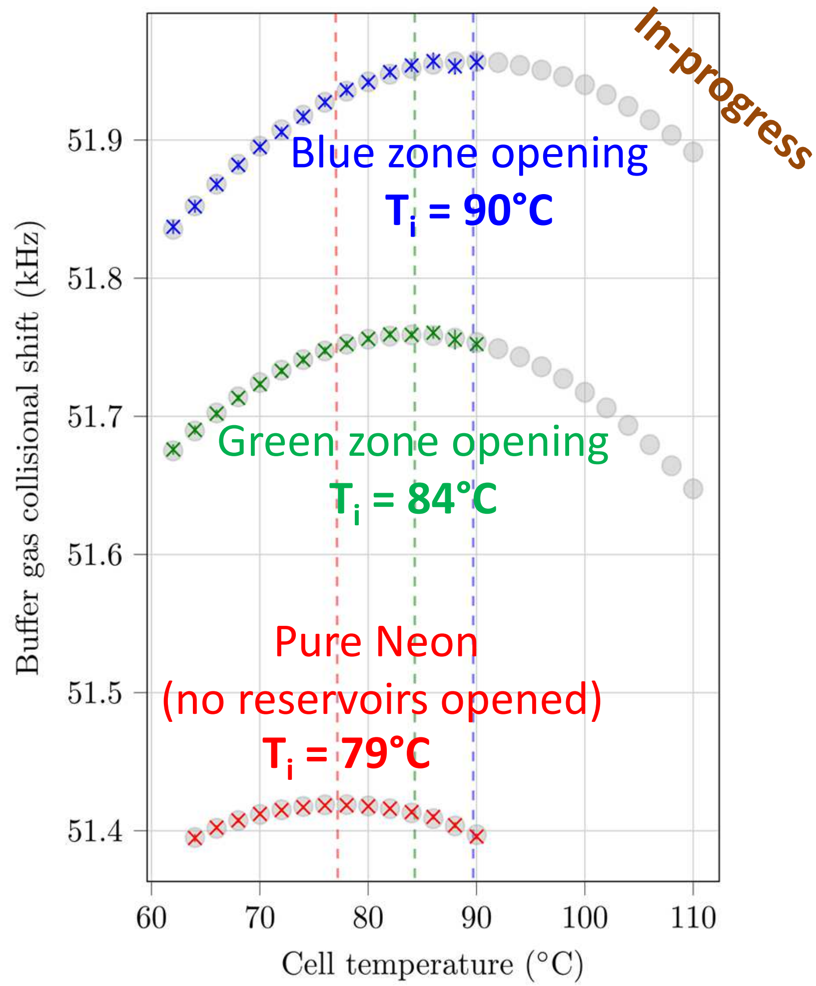

Gradual increase of Helium
Shift of the inversion point with consecutive opening of reservoirs areas
MEMS cells with tunable Ne-He mixture, after wafer sealing

Conclusions on microwave microcell CPT clocks

Microwave CPT-based microcell clocks
low 10^{-12} range stability at 1 day

Ramsey-based interrogation protocols in MEMS cells
Reduction of the clock frequency dependence to laser field parameters by > 100 (Vs CW regime)

Low-permeation glass wafers and Al_2O_3 coatings
Reduction of the He permeation by **450** with ASG glass, by **130** with BSG + Al_2O_3 glass
Reduction of the Ne permeation
Relevant permeation reduction with a 20 nm-thick Al_2O_3 coating

Cells with He-Ne buffer gas mixtures for increased operation temperature
Microfabricated break-seal membranes for fine tuning of buffer gas mixture ratio

-- Perspectives --

Cells with N_2-based buffer gas mixtures
Use of narrow-linewidth VCSELs [1]

[1] M. Huang et al., Appl. Phys. Lett. 121, 114002 (2022)

Towards miniaturized microcell optical references

Probe ultra-narrow transitions
Improve the cell purity

$$\sigma_y(\tau) = \frac{\Delta\nu}{\nu_0}\frac{1}{S/N}\tau^{-1/2}$$

Increase the frequency ν_0
Probe optical transitions
(ν_0 > 300 THz)

Increase the SNR
Low-noise lasers
Detect high-signals

Sub-Doppler spectroscopy techniques

Hot vapor interacts with two counter-propagating fields: Doppler-free resonances

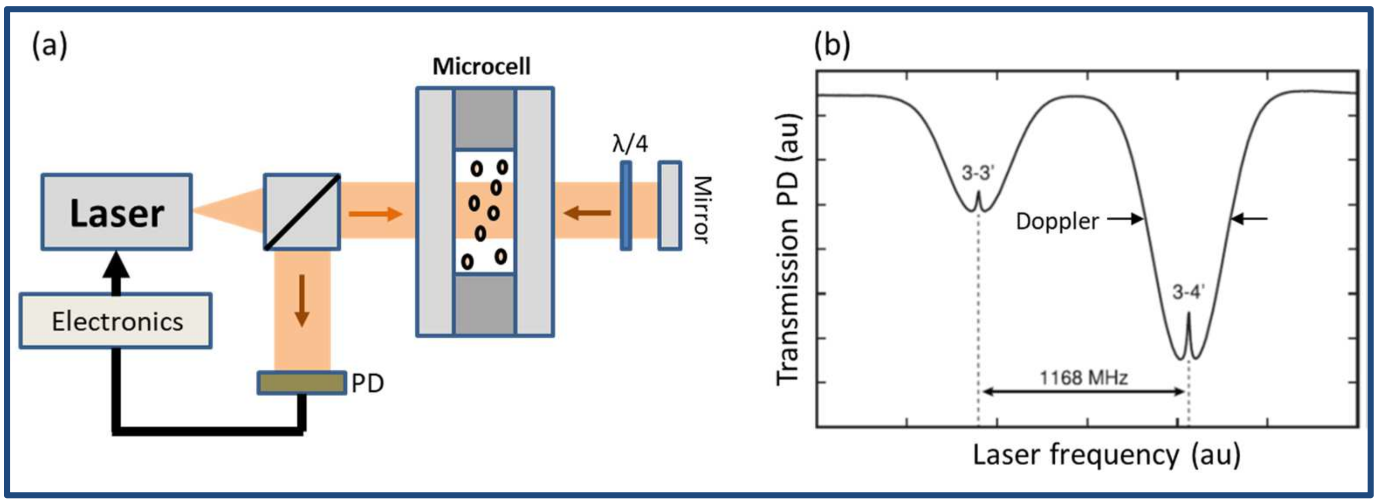

Simple architecture: 1 laser + 1 vapor cell / No laser cooling, no UHV

High potential for miniaturization with MEMS cells and integrated lasers/photonics

Microcell optical references at FEMTO-ST

Dual-frequency sub-Doppler Cs (895 nm)

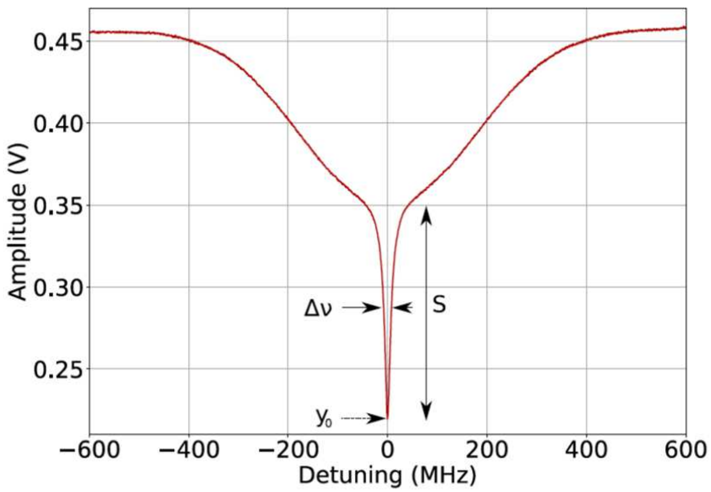

A. Gusching et al., Opt. Lett. 48, 6, 1526 (2023)

Rb two-photon transition (778 nm)

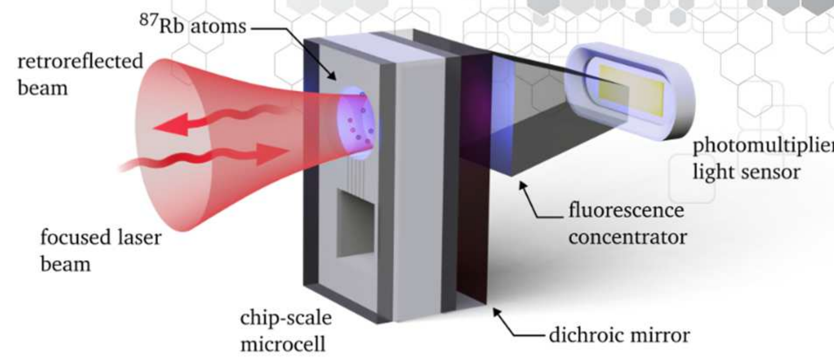

Natural linewidth ~ 330 kHz

M. Callejo et al., https://arxiv.org/pdf/2407.00841 (2024)

Cs atom $6S_{1/2} – 7P_{1/2}$ (459 nm)

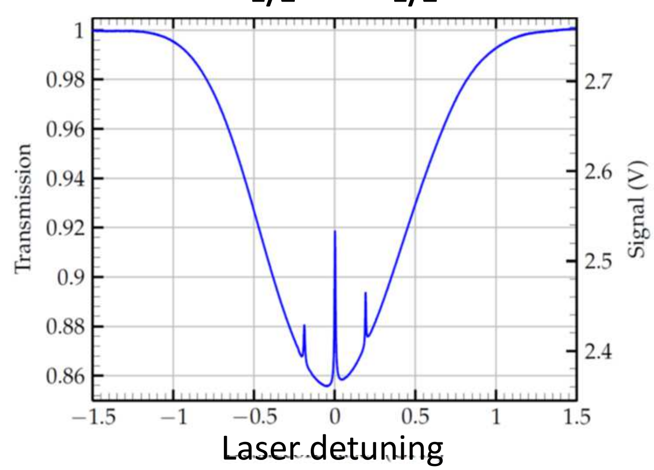

E. Klinger et al., Opt. Lett. 49, 8, 193 (2024)

Rb two photon transition at 778 nm at FEMTO-ST

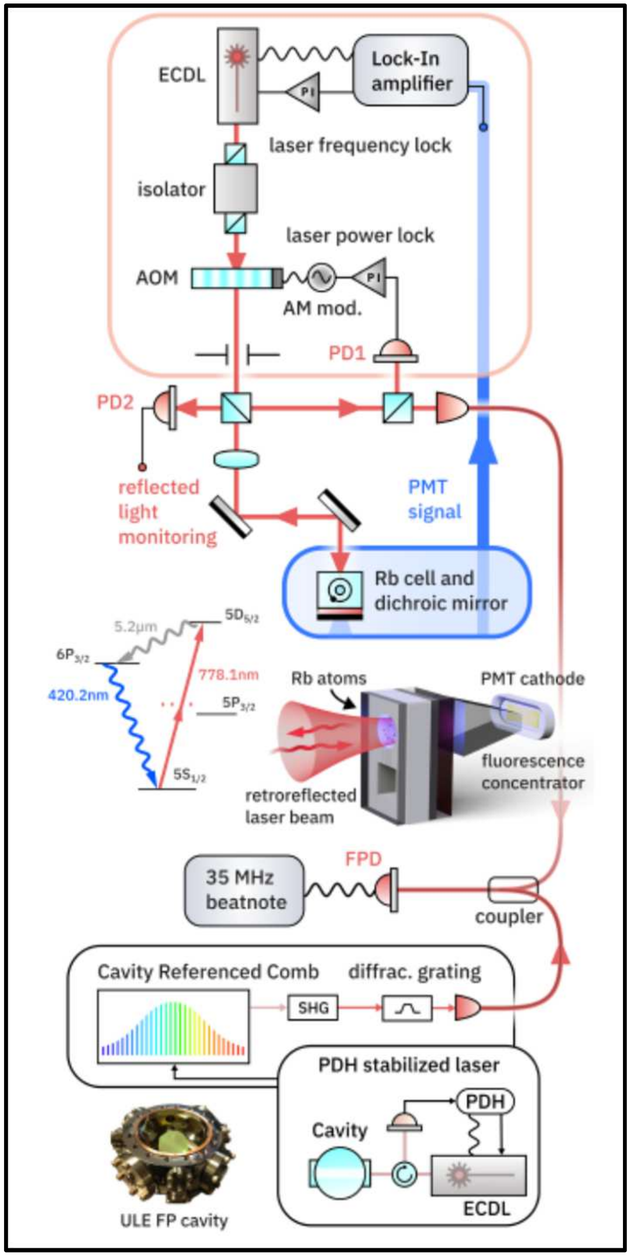

Spectrum in the MEMS cell

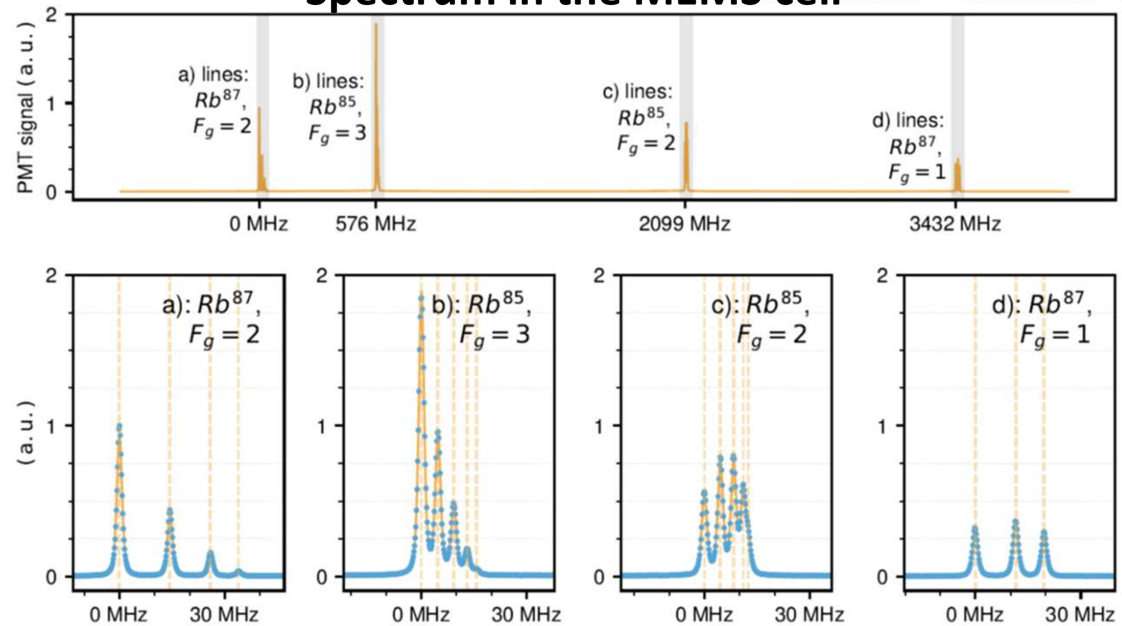

F_g=2, F_e=4 (^{87}Rb)

We worked with this transition

Lorentzian width (MEMS cell) ~ 900 kHz

Collisional broadening due to contaminants

Amplitude of atomic resonance

Laser power

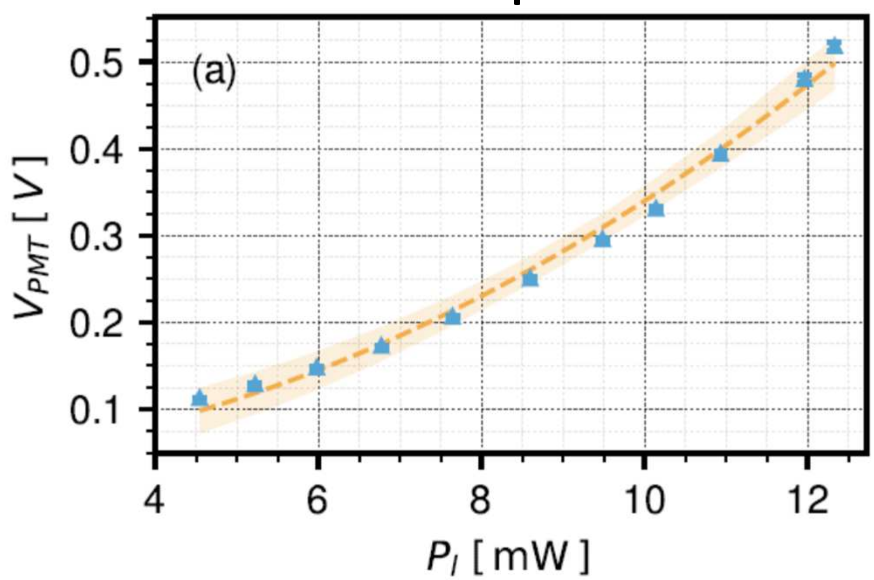

TPA : second-order non-linear process
proportional to the square root of the laser intensity
Behaviour well observed

Cell temperature

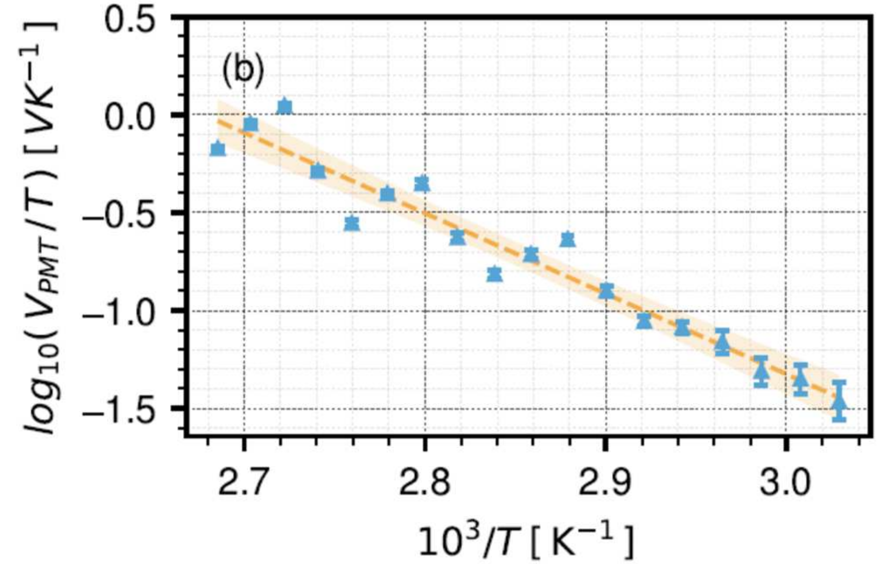

The amplitude of the TPA resonance depends on the vapor density

➡ Operating points : 12 mW (max for our setup), T = 110 °C

Noise sources

Photon shot noise

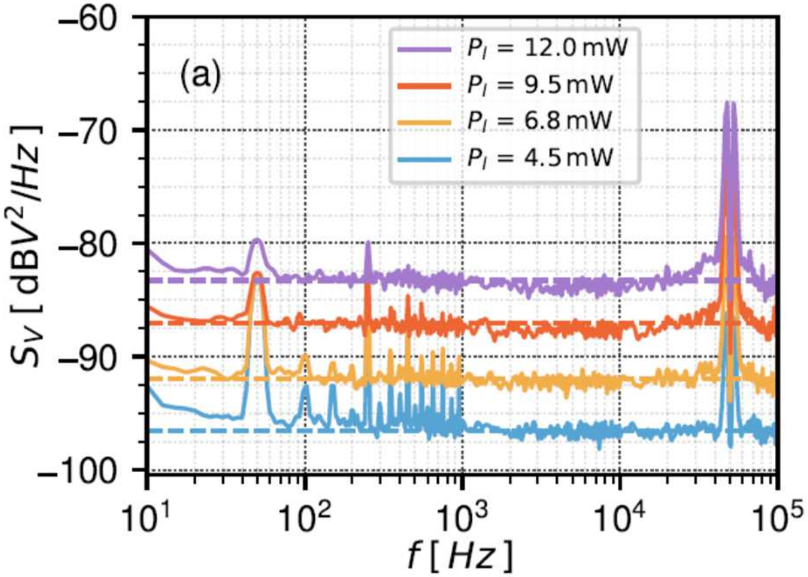

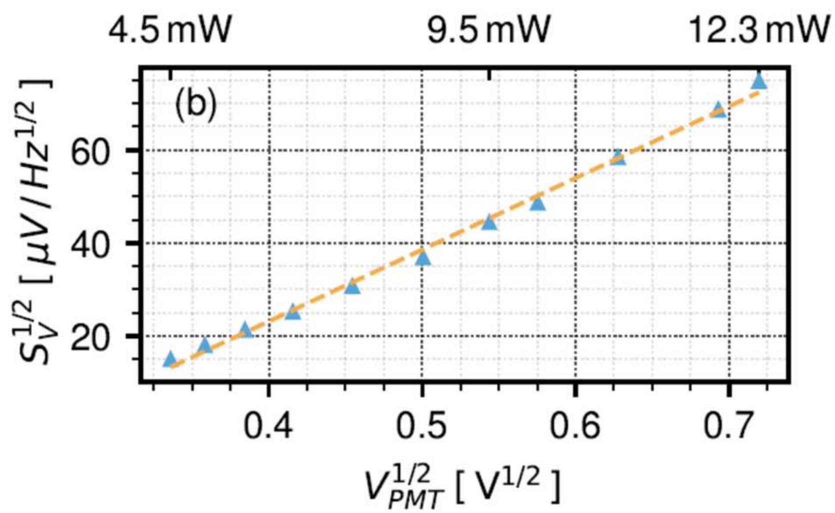

Photon shot-noise limited SNR

Intermodulation noise

$$\sigma_y(\tau) \simeq \frac{1}{2}\sqrt{\frac{S_\nu(2f_m)}{\nu_0^2}}\frac{1}{\sqrt{\tau}}$$

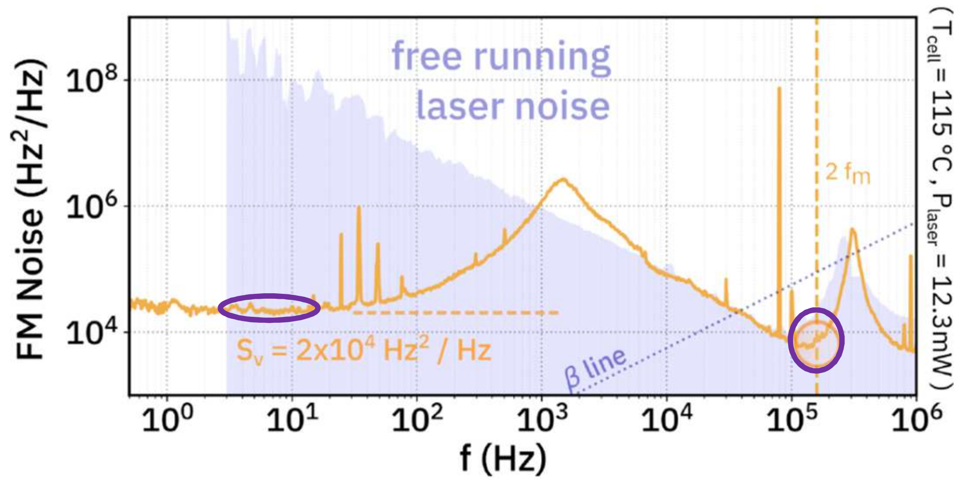

Intermodulation limitation

S_ν = 6000 Hz²/Hz @ 160 kHz

σ_{inter} (1s) = 1 x 10^{-13}

Stability at 1 s (prediction)

S_ν = 2x10⁴ Hz²/Hz @ 1 Hz

σ_y (1s) = 3.5 x 10^{-13}

Short-term stability of MEMS-cell optical references

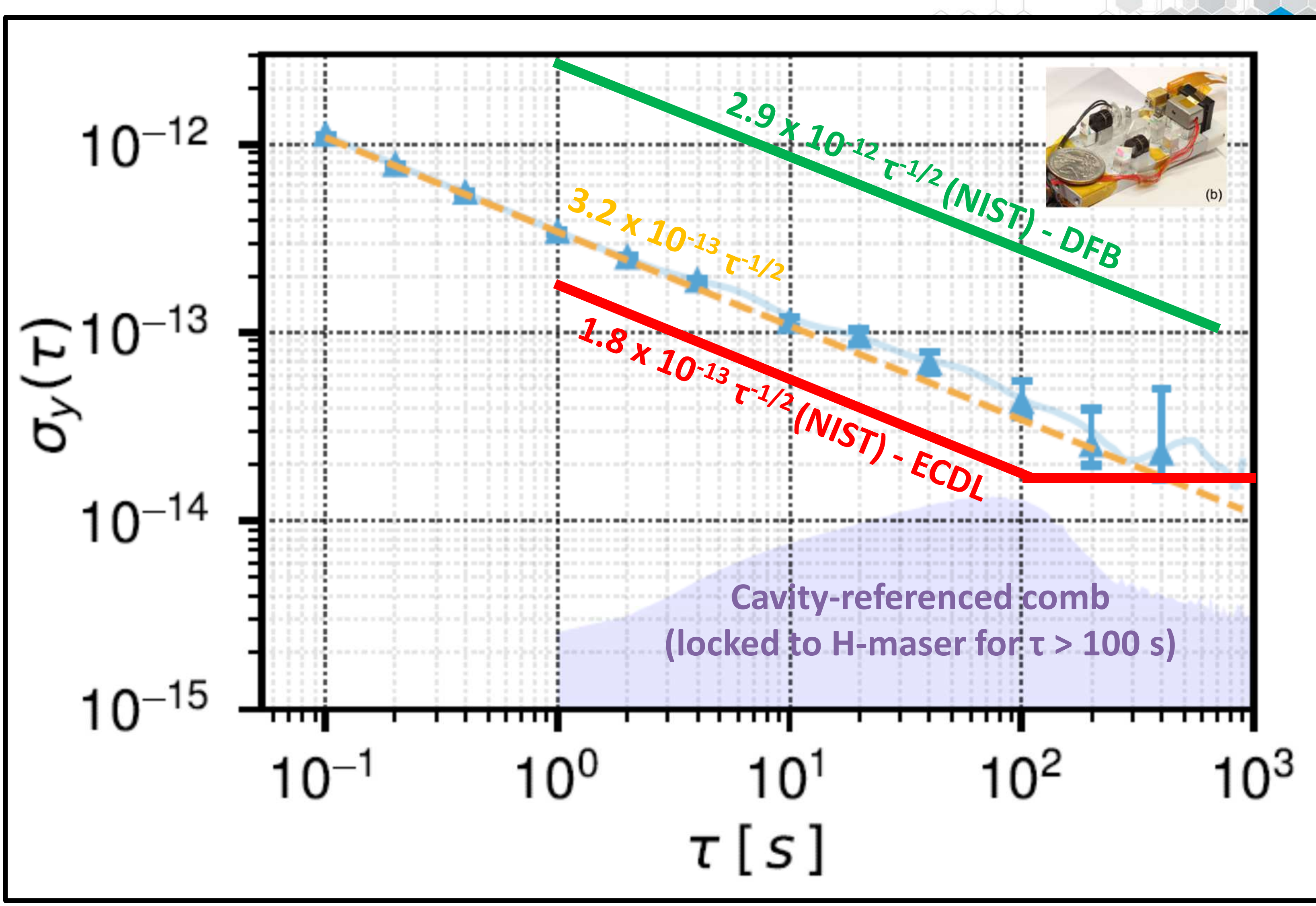

T = 110°C
P = 12 mW
f_m = 80 kHz

M. Callejo et al., https://arxiv.org/pdf/2407.00841

Z. Newman et al., Opt. Lett. 46, 18 (2021) [^{85}Rb transition!]
V. Maurice et al., Opt. Exp. 28, 17, 24710 (2020)

Short-term limits:
Photon shot noise and Intermodulation effect

Frequency shifts

Light-shift (AC Stark) is an important contribution to the mid-term stability of optical references

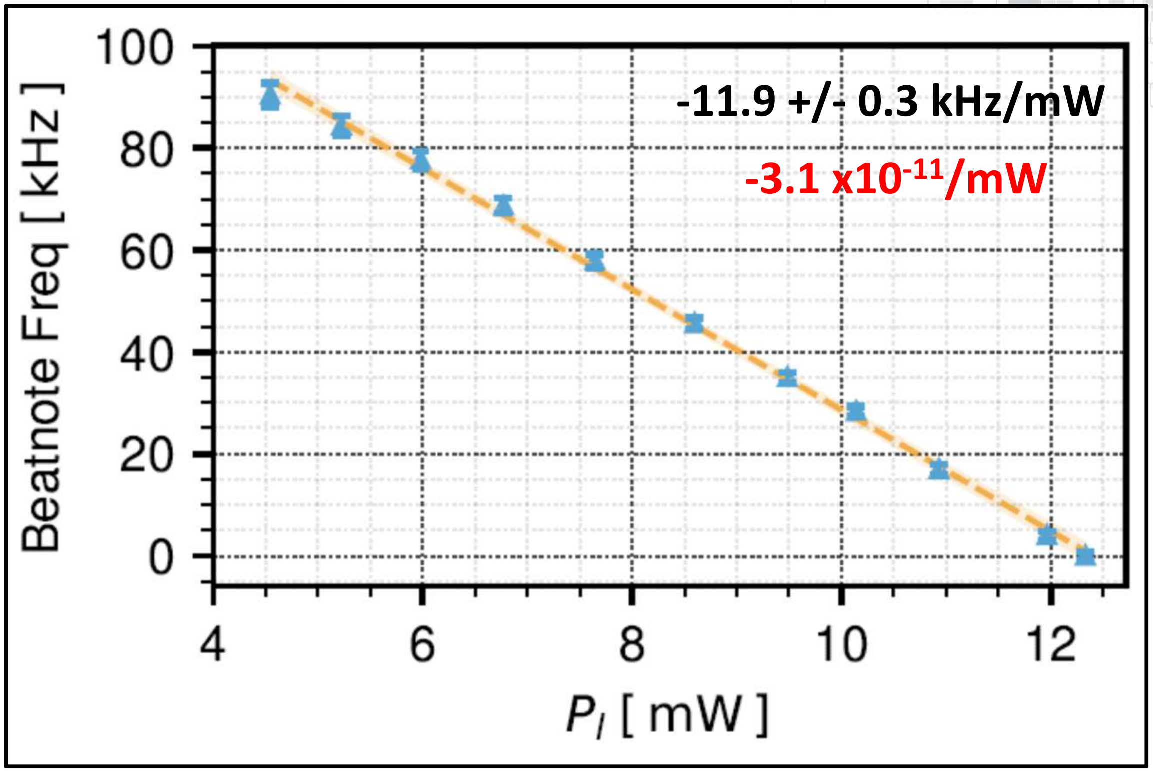

Light-shift mitigation techniques are planned for improved stability > 100 s [1-3]

Collisionnal shifts to be investigated [about - 1 kHz/K measured]

[1] : V. I. Yudin et al., Phys. Rev. Appl. 14, 024001 (2020)
[2]: M. Abdel Hafiz et al., Phys. Rev. Appl. 14, 034014 (2020)
[3] D. Li et al., Opt. Express 32, 2 (2024)

Conclusions on microcell optical references

Microcell optical references: $3.2\times10^{-13}\ \tau^{-1/2}$ up to 100 s
Results obtained with Rb 778 (and Cs 895) experiments

Large margin of progress for optical references
(the 10^{-14} / 10^{-15} range ? at 1 s is realistic)

MEMS cell technology

Ultra-pure MEMS cells
Increased MOEMS functionalities
Optimized collection

V. Maurice et al., Microsyst. Nanoeng. **8**, 129 (2022).
G. D. Martinez et al., Nature Comm. 14, 3501 (2023)
R. Boudot *et al*., Sci. Rep. **10**, 16590 (2020)

Ultra-low noise integrated lasers

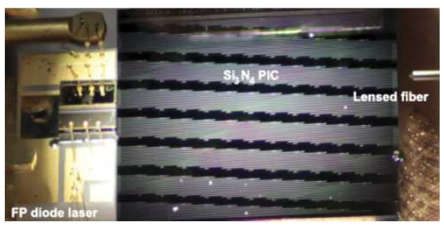

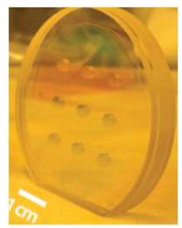

Hybrid photonic-atomic lasers
High-Q micro-resonators
Miniature ultra-stable FP cavities

A. Siddharth et al., APL Photonics 7, 046018 (2022)
G. Lihachev et al., Nature Comm. 13, 3522 (2022)
V. Snigirev et al., Nature 615, 411 (2023)
J. Guo et al., Sci. Adv. **8**, eabp9006 (2022)
C. A. McLemore et al., PRAp **18**, 054054 (2022)
M. Clementi, Light Science Applications 12, 296 (2023)

New regimes

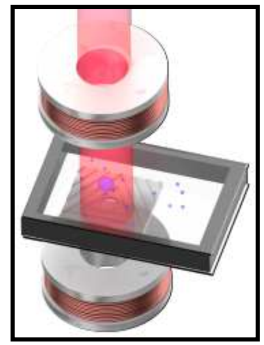

Image credit: J. McGilligan

Cold atoms
Cavity-enhanced interactions

C. C. Nshii *et al*., Nature Nano **8**, 321 (2013)
JP McGilligan *et al*., APL **117**, 054001 (2020)

Thanks to FEMTO-ST colleagues !


R. Boudot


N. Passilly


M. Abdel Hafiz


C. Carlé


R. Vicarini


J. Breurec


C. Rivera Aguilar


E. Klinger


Q. Tanguy


A. Mursa


M. Callejo

Former postdocs & PhD students


S. Keshavarzi,
now in industry
(Germany)

I.Ryger,
now in JILA
(USA)


M. Petersen,
now in Safran
(France)


A. Gusching
now in PTB
(Germany)